Journal of Environmental Chemical Engineering 13 (2025) 119279

Contents lists available at ScienceDirect

Journal of Environmental Chemical Engineering

journal homepage: www.elsevier.com/locate/jece

Sustainable valorisation of waste-derived plastic rich materials into porous carbon materials for adsorption cooling applications

Agata Mlonka-Mędrala [a,*], Małgorzata Sieradzka [b], Wojciech Kalawa [a], Chunfei Wu [c], Marcin Sowa [a], Tomasz Bujok [a], Aneta Magdziarz [b]

[a] AGH University of Krakow, Faculty of Energy and Fuels, Department of Thermal and Fluid Flow Machines, al. A. Mickiewicza 30, 30-059 Krakow, Poland
[b] AGH University of Krakow, Faculty of Metals Engineering and Industrial Computer Science, Department of Heat Engineering & Environment Protection, al. A. Mickiewicza 30, 30-059 Krakow, Poland
[c] School of Chemistry and Chemical Engineering, Queen's University Belfast, Belfast BT7 1NN, United Kingdom

ARTICLE INFO

Keywords:
Porous carbon materials
Adsorption chiller
Waste management
Thermochemical conversion
Chemical activation
Circular economy

ABSTRACT

The thermochemical valorisation of waste materials rich in plastics offers a sustainable approach for waste reduction and the generation of high-value products, aligning with the European Green Deal and circular economy principles. This study investigates the conversion of three solid waste streams: refuse-derived fuel (RDF) from municipal (RDF_MW) and industrial (RDF_IW) sources and tyre-derived fuel (TDF) into activated carbons for application in adsorption cooling systems. A two-step activation process, combining pyrolysis at 600 °C with subsequent steam (850 °C) or chemical (KOH at 800 °C) activation, was employed to enhance porosity and surface area. RDF_IW-derived carbon activated with KOH achieved a maximum BET surface area of 955 m^2/g, while methanol adsorption tests showed an uptake exceeding 40 %. Heavy metal analysis revealed significant Zn contamination in TDF (up to 37,415 mg/kg), while Cr, Pb, and Sn were prominent in RDF samples; chemical activation reduced Zn content by up to 70 %. Performance testing in methanol-based adsorption chillers showed that RDF_IW_H2O and RDF_IW_KOH samples achieved specific cooling powers (SCP) of 53.5 W/kg and 88.9 W/kg, and coefficients of performance (COP) of 0.631 and 0.673, respectively, comparable to commercial activated carbons (CWH-22: SCP = 95.5 W/kg, COP = 0.615). These findings demonstrate the dual benefit of valorising heterogeneous waste into functional sorbents while enabling energy-efficient, low-grade thermal cooling systems.

1. Introduction

The growing challenges of climate change, driven by rising CO_2 emissions, the depletion of fossil fuels, and environmental degradation associated with economic development, highlight the urgent need for sustainable energy solutions. Since modern energy generation and industrial activities still rely heavily on large-scale fossil fuel combustion, it is crucial to reduce human-induced CO2 emissions to mitigate the worsening impacts of global warming [1]. Addressing resource demands while minimizing emissions and waste is critical [2]. In this context, the circular economy (CE) offers a systemic framework for recovering energy, extending material life cycles, and minimizing environmental impacts. The focus is on optimizing resources, preserving value, and eliminating waste sustainably [3]. Developing activated carbons (AC) from waste aligns with CE principles and supports the EU's Clean Energy goals for 2030 and 2050 by reducing waste incineration and promoting low-emission technologies such as gasification and pyrolysis.

The significance of waste-derived activated carbon (AC) extends beyond traditional environmental applications. The use of AC synthesised from biomass residues, waste wood, or industrial by-products contributes to resource efficiency and the valorisation of waste streams, thereby adding value within the circular economy (CE) framework, alongside the use of waste-to-energy technologies. Activated carbon can be produced from materials obtained through high-temperature carbonization processes. Materials derived from biomass via thermochemical processes, such as gasification or pyrolysis, are referred to as biochar. This material is notable for its broad range of applications due to its wide availability, structural stability, high carbon content, and renewability [4]. As a result, using biomass for AC production is highly justifiable. However, further activation is needed,

* Corresponding author.
E-mail address: amlonka@agh.edu.pl (A. Mlonka-Mędrala).

https://doi.org/10.1016/j.jece.2025.119279
Received 25 July 2025; Received in revised form 3 September 2025; Accepted 13 September 2025
Available online 14 September 2025

which can be achieved through physical methods like steam, air, or CO_2 gasification and pyrolysis processes, or through chemical methods that use hydroxides, such as KOH or NaOH, or other activation agents like $ZnCl_2$, $FeCl_3$, or H_3PO_4 [5–7]. The choice of activation method is crucial, as it significantly affects the material's textural properties and, consequently, its potential applications [8,9].

Activated carbons have significant potential for various industrial applications, including air [10] and water purification [11], gas separation, and catalysis processes [12]. An emerging and important application for activated carbons is in adsorption cooling, where they can serve as sorbents for refrigerants such as ammonia or methanol [13], facilitating the production of ice water. This underscores the growing importance of activated carbons in adsorption chillers [13]. Their favourable thermal conductivity and diffusivity further enhance their performance in these systems, allowing them to act as conductive matrices for advanced sorption composites, such as metal-organic frameworks [14]. Overall, this positions activated carbons at the forefront of sustainable cooling technologies.

However, several challenges hinder the large-scale use of waste-derived activated carbons in adsorption cooling systems. One major concern is the contamination from heavy metals that may originate from the raw materials used in production. These contaminants can stem from the waste feedstock itself [15]. Therefore, it is essential to implement rigorous quality control and purification protocols to reduce heavy metal contamination in activated carbons synthesised from waste materials.

Recent research has significantly advanced the techniques for synthesising activated carbon (AC) and expanded their application range. However, systematic studies on waste-based precursors for adsorption cooling remain limited. In this study, we evaluated activated carbons derived from waste materials, specifically waste tires and refuse-derived fuel (RDF), alongside commercial activated carbons, to assess their potential as sorbents in adsorption cooling systems. The materials selected for this study adhered to the principles of circular economy (CE) and the European Union waste hierarchy. They were processed through waste-to-energy technologies, such as pyrolysis and gasification, to produce new forms of energy (like gas or oil), while simultaneously utilizing the solid residue to create activated carbon. The sorption properties, contamination profiles, thermal stability, and surface morphology of the materials were systematically characterised to determine their viability for incorporation into sorption cooling systems. A critical aspect of these sorption studies is the choice of adsorbate. In this case, it was chosen methanol, as it is commonly used in activated carbon-methanol systems. An added advantage of the activated carbon-methanol pairing is its low-temperature desorption requirement, allowing for the use of waste heat generated from various production processes [16].

This research introduces innovative contributions by integrating circular economy (CE) strategies with adsorption cooling (AC) technologies in two significant ways. First, it valorises waste-derived materials by transforming them into functional adsorbents for sustainable cooling applications. Second, it provides a comparative assessment of various waste precursors against commercial alternatives, which aids in identifying performance trade-offs and challenges. These systems present a sustainable solution to the increasing electricity demand for air conditioning, especially in the context of climate change [17,18]. Although the application of AC in adsorption chillers is an expanding area of research [19], several challenges persist. These include the necessity for improved materials with better adsorption properties [20], enhanced mass and heat transfer in heat exchangers [21], efficient recovery mechanisms [22], and the need to extend the life cycle of these systems [23].

Despite the growing interest in the application of activated carbons (AC) in adsorption cooling systems, significant knowledge gaps remain regarding both their synthesis from waste precursors and their performance under methanol working conditions. Previous studies have mainly focused on environmental remediation and conventional sorption uses, whereas adsorption chillers pose new research challenges. These include: (i) the presence and chemical stability of contaminants, especially heavy metals, (ii) the need to design pore structures that enable efficient heat and mass transfer, (iii) chemical compatibility and long-term cyclic stability with methanol, and (iv) the development of activation procedures that yield ACs with tailored porosity, enabling desorption at regeneration temperatures below 80 °C and thereby improving the COP of the process. In particular, the potential of refuse-derived fuel (RDF) and end-of-life tyres as precursors for ACs with the required properties for adsorption cooling remains largely unexplored.

This study provides a novel contribution by combining thermochemical processing with advanced sorption technology to valorise challenging waste streams into high-value adsorbents. The analysis of steam and KOH activation effects on pore structure and methanol sorption compatibility delivers new insights into both the potential and the limitations of waste-derived ACs in adsorption cooling. Importantly, the research integrates a fundamental and an applied dimension: based on multiple vacuum sorption–desorption cycles of the synthesised ACs, theoretical COP and SCP values for selected working pairs were estimated, offering a rapid and efficient prototyping method for sorbents dedicated to cooling applications. Thus, the work highlights a dual benefit: waste valorisation and the development of low-emission cooling technologies, contributing directly to the EU's clean energy transition and circular economy goals.

2. Materials and methods

2.1. Materials

The present study is a comparative analysis of porous carbon materials obtained from waste materials: tyre derived fuel - TDF, refuse-derived fuel – RDF, RDF obtained from municipal solid waste – RDF_MW and RDF obtained from industrial waste - RDF_IW, and commercial activated carbons available on the Polish market: AKPA-22 and CWH-22 delivered by Gryfskand Company. First, AKPA activated carbon is produced from hard coal and beetroot molasses, whereas CWH activated carbon raw material is charcoal.

2.2. Porous carbon materials synthesis

To develop a porous structure in the waste-derived materials, a two-step activation procedure was employed, consisting of an initial pyrolysis step to produce char, followed by activation using either physical or chemical methods.

2.2.1. Pyrolysis - first stage thermochemical treatment of raw feedstock

The pyrolysis process was conducted in an inert gas atmosphere, with nitrogen at a flow rate of 80 ml/min serving as the process gas at a temperature of 600 ºC and a process time of 30 min. The process parameters were selected based on previous experience and ongoing experimental studies on the pyrolysis process in the temperature range from 300 to 600 °C [24,25]. The waste material was subjected to a slow pyrolysis process (stepwise heating of a small-scale horizontal fixed-bed reactor) that promotes the formation of both gas and solid phases. Both the pyrolytic gas and the extracted solid fraction – char, were analysed for their composition. The liquid fraction was not extracted during the experimental studies, due to the horizontal design of the reactor and the low proportion of the liquid fraction in the process products.

2.2.2. Physical activation – second stage thermochemical treatment using steam gasification

Subsequently, the char undergoes steam activation at 850 °C using a semi-batch vertical quartz reactor. The gasification of chars occurred under a steam atmosphere at 850 °C. Steam was injected into the pre-heated reactor at 300 °C, and nitrogen was introduced into the reactor as a carrier gas. Approximately 1 g of char was placed inside the quartz

tube reactor. The sample was placed on glass wool and stainless-steel mesh to prevent movement along the reactor. The gasification process was conducted for 25 min. The initial heating stage, which lasted for 15 min, was used to reach the set temperature of 850 °C. This was followed by a 10 min gasification stage at selected process temperature. The flow of gasification agents was set to 1 ml/min of water vapor and 80 ml/min of N_2. The agents were directed through the reactor where gasification occurred, with the process gases subsequently moved into a liquid receiver placed in an ice bath for condensable gases collection. Permanent gases were directed through a dryer and collected in a Tedlar bag for syngas analysis using a GC gas analyser. In this study, gas collection started after the reactor reached 500 °C.

2.2.3. Chemical activation – second stage thermochemical treatment using KOH activation

Activation of the chars obtained in the pyrolysis process was carried out through a chemical activation process using KOH as an activating agent. The activation process was performed in a horizontal fixed-bed reactor. The process parameters were as follows: activation temperature 800 ºC, activation time 1 h, nitrogen atmosphere with a flow of 80 ml/min, and mass ratio of char to KOH 1:3. The mixture of char and hydroxide was ground in a knife grinder prior to thermal treatment to homogenize the sample. After activation, the activated carbons were subjected to repeated rinsing in distilled water to remove KOH, and then the obtained activated carbons were dried at a temperature of 105 ºC for a minimum of 6 h and tested for their adsorption properties.

2.3. Sample characterisation

2.3.1. Analytical methods used in the study – characterisation of synthesis gas from pyrolysis and steam gasification

The gas phase obtained from both the pyrolysis and gasification procedures were collected and analyzed using an Agilent Technology 7890 A GC gas chromatography system. Various gases including CH_4, CO_2, O_2, CO, C_2H_6, C_2H_4, C_2H_2, and H_2 were detected at different concentrations. This GC system featured TCD (thermal conductivity) and FID (flame ionization) detectors. The analysis process was carried out using an appropriately designed programme that allowed the separation of all components of the test gas.

2.3.2. Analytical methods used in the study – feedstock and porous carbon materials characterisation

Simultaneous thermal analysis (STA) was conducted for raw feedstock using Mettler Toledo TGA/DSC 3 + . Samples were tested in aluminium oxide crucibles, and a constant heating rate of 10 °C/min was used in 50 ml/min nitrogen.

To analyse thermal degradation and modification of material through thermal treatment methods additional ultimate analysis was done for raw feedstock, obtained chars and steam activated porous carbon materials. Carbon, hydrogen and nitrogen contents were determined using Truspec CHN628 Leco analyser.

Porous carbon materials obtained in this study, along with commercial activated carbons, were examined using a scanning electron microscope equipped with an energy-dispersive X-ray detector (Nova NanoSEM 450) to characterise their morphology and porosity. For the morphological analysis of the activated carbons, an accelerating voltage of 2 kV was applied.

Fourier transform infrared spectroscopy (FTIR) was employed to identify the chemical functional groups present in the samples under investigation. This technique provides information revealing specific chemical bonds and molecular structure based on the vibrations of chemical functional groups. In these analyses, the Bruker Alpha II instrument was employed to study the collected spectra within the range of 400–4000 cm^{-1}.

Inductively Coupled Plasma Optical Emission Spectroscopy (ICP-OES) was used for detection of heavy metals in raw feedstock and activated samples by accredited laboratory Energopomiar Gliwice. The concentration of the following elements was determined: As, Cd, Co, Cr, Cu, Mn, Ni, Pb, Sb, V and Zn. Solid samples prior analysis were mineralized in acid mixtures. Mercury content was determined using Atomic absorption spectrometry with amalgamation technique.

Structural properties were determined using a low-temperature gas adsorption method. Micromeritics ASAP 2020 volumetric analyser was used, it operates at low-pressure nitrogen adsorption at a temperature of 77.35 K with a relative pressure range of $0<P/P_0<0.996$. The Brunauer-Emmet-Teller (BET) method was used to determine the specific surface area of the activated carbons and the average diameter of the pores based on the adsorption isotherms with p/p_0 ranging between 0.06 and 0.20; both adsorption and desorption curves were used. The pore diameter measurement also considered the presence of the adsorbed layer.

The methanol sorption properties of the activated carbons in this study were assessed using a dynamic vacuum gravimetric system (DVS Vacuum), employing methanol as a widely recognized non-hazardous adsorbate for working pairs with activated carbon [13,26–28]. The measurement protocol consisted of 22 sequential stages. The given amount of the investigated material was first collected and weighed on a precision balance to ensure a comparable mass across all experiments. Each sample was then placed in an identical crucible to maintain measurement reproducibility. Measurements were performed using the DVS Vacuum apparatus, which offers high precision: the sample mass is recorded with an accuracy of 0.1 μg, and the temperature is controlled with an accuracy of 0.1 °C, ensuring highly reliable data. Initially, the samples were dried and degassed by heating both the apparatus and the sample to 100 °C for 60 min. This was followed by a one-hour stabilization phase at the desired process temperature. For each sample, measurements included three stable adsorption-desorption cycles to detect any potential anomalies and to evaluate the reproducibility of the sorption behaviour. In summary, the evaluation of results is based on precise sample weighing, conducting measurements with high accuracy, and consistently following the same procedure, which includes multiple measurement cycles, thereby ensuring reproducibility and reliability of the data.

The materials were evaluated at two process temperatures, 30 °C (adsorption) and 60 °C (desorption), as previous studies have demonstrated that intermediate temperatures exert minimal influence on the sorption behaviour of activated carbons [29]. These conditions enabled a comprehensive assessment of the adsorption dynamics and performance characteristics of the materials, with a view toward their potential application in adsorption chillers driven by low-temperature waste heat.

The surface area of the samples was determined using the BET model. The standard BET equation was applied:

$$\frac{1}{V}\frac{x}{1-x}=\frac{c-1}{cV_m}x+\frac{1}{cV_m}$$

where:

x – the partial pressure of methanol vapor above the surface,

V – the amount of adsorbed vapor.

The plot of (1/V) [x/(1 −x)] as a function of x yields a straight line. From the slope and intercept of this line, V_m, i.e. the amount of gas adsorbed in the case of monolayer formation, and the constant c, related to the strength of the adsorbate-adsorbent interaction, are determined.

3. Results and discussion

3.1. Characterisation of synthesis gas from pyrolysis and steam gasification

During the experimental process, pyrolytic gas and syngas were collected in two distinct stages: the initial carbonization phase, also

known as pyrolysis, and the subsequent activation stage involving steam gasification. These stages are critical for understanding the composition and energy potential of the gases produced. The detailed results of the gas composition analysis obtained from both phases are presented in Fig. 1a) and b). It is important to note that nitrogen, used as the carrier gas throughout the procedure, does not participate in the chemical reactions and serves solely as an inert ballast. Therefore, it was intentionally excluded from the final calculations to ensure accurate representation of the reactive and energy-relevant gas components.

Fig. 1a) shows an analysis of the composition of the pyrolysis gas. The results of the chromatographic analysis show that the main component, in all cases, is methane (CH_4). The highest methane content of 51.48 % and hydrogen content of 22.70 % were recorded for the fuel sample produced from used tyres. This raw material also had the highest carbon content, resulting in the highest-quality pyrolysis gas. Also in this case, the lowest CO and CO_2 contents were recorded, further enhancing the quality and value of the pyrolysis gas. A significant amount of higher hydrocarbons (14.73 %) was recorded in the pyrolysis gas for the used tyres, but the amount collected was too small to be analysed further. The results presented for the fuel produced from used tyres are consistent with those for the same type of fuel, but on an enlarged laboratory scale [30].

The two RDF samples, one produced from industrial waste (RDF_IW) and one from municipal waste (RDF_MW), gave similar results, as their elemental composition was similar. However, RDF_IW had a higher carbon content, which resulted in higher methane concentrations in the pyrolytic gas produced. In addition, the high content of organic matter, mainly organic waste, in the fuel sample produced from municipal waste resulted in high CO_2 and CO emissions of the pyrolytic gas [31]. In particular, the biodegradable fraction present in the alternative fuel is responsible for the high carbon dioxide emissions in the pyrolytic gas [32]. The composition of the pyrolysis gas is influenced not only by the composition of the feedstock, but also by the process temperature, the reactor design, the reactor heating rate and the residence time of the material at the set process temperature [33].

The results of the synthesis gas analysis shown in Fig. 1b) indicate that hydrogen is the main constituent. The results obtained confirm that, using the steam gasification method, it is possible not only to obtain a solid product with a developed porous structure, but also a synthesis gas rich in H_2. Nearly 70 % hydrogen in the gas product was recorded for RDF carbonate produced from industrial waste. In contrast, methane and higher hydrocarbons were collected in trace amounts. A very interesting behaviour was recorded for the fuel obtained from used tyres. In the literature, TDF fuel is presented as a material suitable for activation, but during steam activation a very high thermal degradation of the material was observed, as up to 53.38 % of the synthesis gas was CO_2. Furthermore, this resulted in poor activation results, low active surface area and sorption properties towards methanol of the obtained porous material. The high CO_2 content and low CO concentration in this case may be related to the carbon monoxide/water vapour conversion reaction ($CO + H_2O \rightarrow CO_2 + 3\ H_2$) [34], in which CO and water vapour are the reactants, while CO_2 and H_2 are the products. Therefore, the appearance of carbon dioxide in the process gas or synthesis gas favours hydrogen formation [35].

The verification of the gas composition allows to calculate related lower heating value (LHV) of obtained syngas. The calculation was provided based on the following equation: $LHV = ([H_2]\bullet 107.98 + [CO]\bullet 126.36 + [CH_4]\bullet 358.18 + [C_2H_2]\bullet 56)/1000$, MJ/Nm^3 [36] and obtained results are presented in Table 1. The assumptions that syngas was composed of H_2, CO, CH_4 and C_2H_2 have been made in order to standardize the results and make them comparable with each other. The LHV value varies from 21.6 MJ/Nm^3 to 19 MJ/Nm^3 after pyrolysis process, where this value varies from 10.4 MJ/Nm^3 to 5.3 MJ/Nm^3 after gasification. This phenomenon is related to the fact that part of the volatiles was released during pyrolysis. The analysis of the syngas composition confirms this, as the content of the most calorific component of syngas, i.e. CH_4, decreased from the range of 51.5 % — 25.5 % for the pyrolysis process to the range of 1.1 % — 0.4 % for the gasification process.

3.2. Thermal decomposition of raw feedstock

Thermal decomposition under a nitrogen atmosphere was analysed to determine the most suitable temperature for the pyrolysis process at a lab-scale test rig. TG, DSC, and DTG curves are presented in Fig. 2.

TG analysis of RDF and TDF raw fuels in an inert gas (nitrogen) atmosphere allowed a preliminary determination of the properties of the materials studied and the temperature of the pyrolysis process carried out on a laboratory scale. Moisture release was observed at low temperatures, as in all cases, the first pick was observed before reaching 150 °C. Complete decomposition of the material was observed above 550 °C, allowing the selection of a pre-treatment process temperature of 600 °C. Further increases in temperature are usually associated with evaporation and thermal decomposition of inorganic matter [37].

In the DTG plot shown in Fig. 2, two main peaks are observed related to the thermal decomposition of the organic matter contained in the RDF_IW and RDF_MW. Based on the characteristic thermal decomposition temperatures of the different waste fractions, it can be concluded that both the municipal and industrial waste-derived RDF samples were characterised by fractions with similar composition and properties.

For the pyrolysis of the waste fuel from tyres, one main peak was observed representing the thermal decomposition of natural rubber, in the range of 300–500 °C. The slight weight loss observed at lower

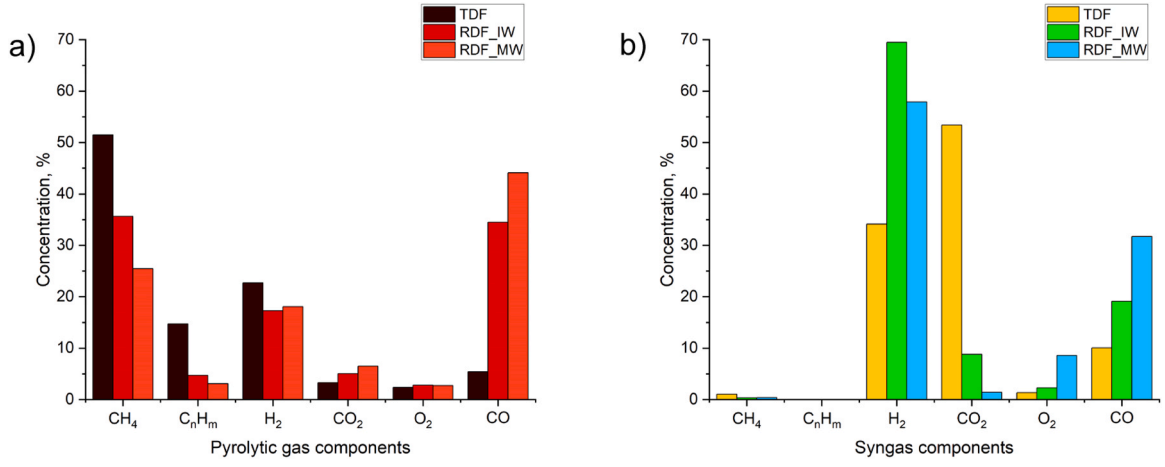

Fig. 1. Analysis of synthesis gas from: a) first stage carbonization process, and b) steam gasification.

Table 1
The LHV of the syngas produced during the pyrolysis (P) and gasification (G) processes.

Sample	TDF_P	TDF_G	RDF_IW_P	RDF_IW_G	RDF_MW_P	RDF_MW_G
LHV, MJ/Nm^3	21.6	5.3	19.0	10.0	16.7	10.4

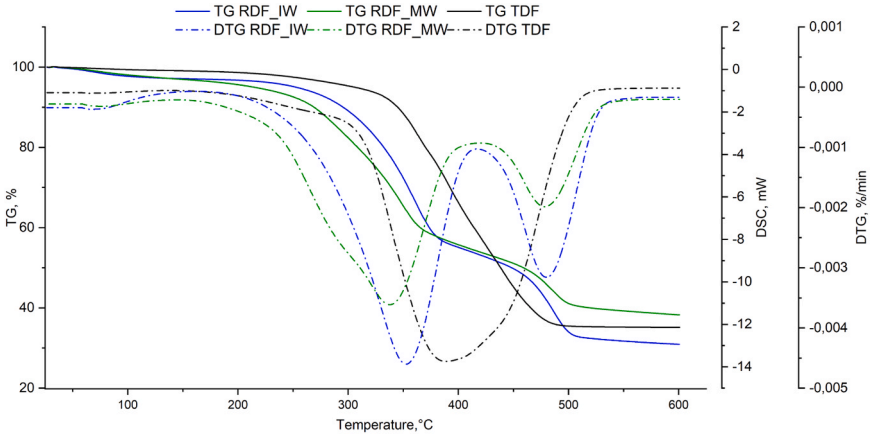

Fig. 2. Thermal behaviour of waste materials up to 600 °C under inert atmosphere.

temperatures, from about 200 ºC onwards, is related to the thermal decomposition of organic additives, a component of a tyre [37].

3.3. Proximate analysis of the raw feedstock and produced chars after the pyrolysis process

Elemental analysis of raw feedstock showed that the highest carbon content was noted for the waste tyres sample, whereas the highest content of hydrogen was determined for RDF derived from industrial waste (Table 2).

The fuel obtained from used tyres had more than 80 % of carbon in raw feedstock, while RDF fuels had approximately 20–30 % lower carbon content in the raw sample. In general, rubber waste from tyre machining is characterised by a homogeneous composition and a high carbon content [38]. In thermal and chemical treatment processes to produce porous carbon materials, tyre samples are subject to preliminary mechanical processing and steel elements, and textile fibres are removed from them [39].

The alternative fuel produced from municipal waste had a lower carbon content than the fuel obtained from industrial waste, and both samples had a similar hydrogen content. The significantly higher nitrogen content in the RDF_MW sample resulted from the properties of municipal waste from which this material was produced. Municipal waste, mainly from individual recipients, consists mainly of biodegradable waste with a higher nutrient content, such as nitrogen [40,41]. Alternative RDF fuels, however, are characterised by high heterogeneity and their composition is very diverse. RDF fuel includes fractions such as plastic with a carbon content of 60–90 %, depending on its type, paper with a carbon content of about 40 % and textiles containing about 50 % carbon [33,42]. The fractional composition depends on the place of production, the composition of raw waste, the installation used for its pre-treatment and the requirements set by recipients of alternative fuel. Depending on demand, mixtures are prepared with higher or lower caloric value and different permissible concentrations of contaminants [43,44].

After the initial thermal treatment by pyrolysis, a significant reduction in carbon content was observed in the char derived from tyre-derived fuel (TDF). This was directly reflected in the composition of the pyrolysis gas, which was enriched in methane and higher hydrocarbons, indicating efficient volatilisation of carbonaceous fractions. In contrast, the chars obtained from refuse-derived fuels (RDF) exhibited only minor changes in carbon and nitrogen contents after pyrolysis. This trend correlates with their gas composition, which contained higher proportions of CO, suggesting a more balanced consumption of carbon and oxygen and leading to comparatively moderate changes in the elemental composition of the resulting chars in relation to the raw feedstocks. During the subsequent steam gasification step, extensive CO_2 release was observed for the TDF sample, which was accompanied by a relative increase in carbon concentration in the residual solid phase. For the RDF-derived samples, however, a greater degree of carbon consumption was evident. This behaviour can be attributed to the carbon–steam reforming reaction ($C + H_2O \leftrightarrow CO + H_2$), further enhanced by partial combustion processes and the heterogeneous character of RDF, which promotes more extensive conversion of the solid matrix.

Table 2
Proximate analysis of raw feedstocks and chars collected after pyrolysis (P) and steam gasification (H2O_850) processes.

Sample\Element	C, wt%	H, wt%	N, wt%
TDF	81.82	7.48	0.52
P_TDF	62.31	0.78	0.38
TDF_H2O_850	69.21	0.16	0.31
RDF_IW	57.24	7.59	2.00
P_RDF_IW	59.34	2.58	3.02
RDF_IW_H2O_850	44.47	0.78	0.79
RDF_MW	49.40	6.65	1.29
P_RDF_MW	47.42	1.73	1.73
RDF_MW_H2O_850	44.63	0.96	0.81

3.4. Structural and morphological analysis of produced activated carbons

The structural and morphological characteristics of activated carbons were examined using scanning electron microscopy (SEM). The morphologies of two commercial activated carbon and five synthesised samples are presented in Fig. 3.

The commercial samples AKPA-22 and CWH-22 were characterised by a similar regular porous structure. The morphology of these samples was homogeneous, and a honeycomb-like structure can be observed. The presence of macropores with a diameter of a few micrometres allows the development of a deeper microporous structure of the activated carbon, and a mesoporous structure of the adsorbents is visible in the

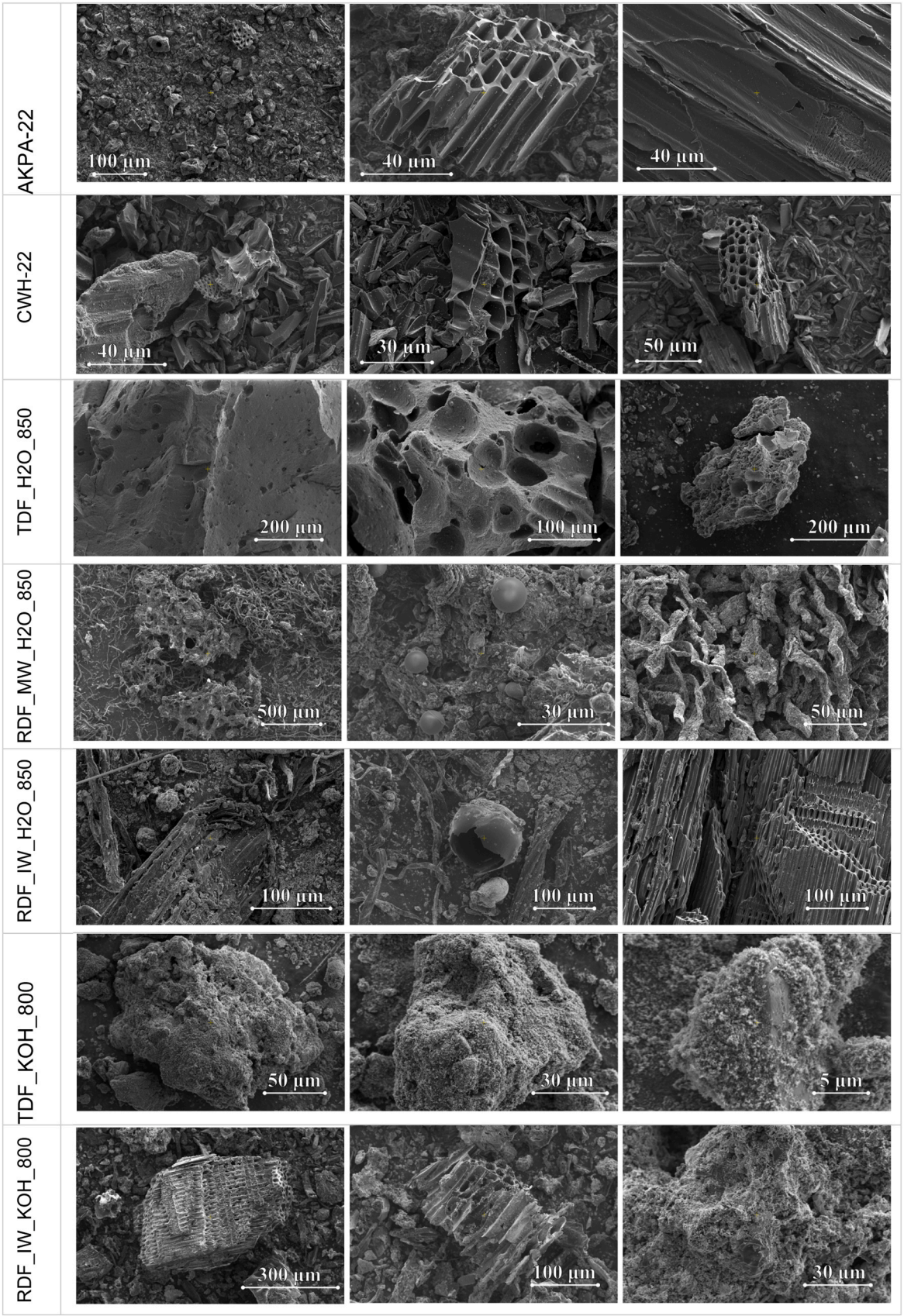

Fig. 3. Morphology analysis of commercial activated carbons and of synthesised porous carbon materials.

images taken at high magnification.

Investigations of the morphology of synthesised porous carbon materials allow a preliminary determination of the porous structure developed during processing. In the case of materials synthesised from waste fuels, this is a key parameter allowing verification of the influence of the synthesis process parameters on the development of the porous structure.

The images revealed the formation of macropores in the steam-activated used tyres, with a limited number of mesopores (see Fig. 3 TDF_H2O_850). The expected porous structure for this type of fuel, obtained by steam activation of the pyrolysis-derived char, is a mesoporous structure [39]. However, this could not be observed in the taken photographs. One significant benefit of this waste material over alternative fuels such as RDF and SRF is its high degree of homogeneity, particularly after the removal of metal elements from the raw material. However, the rubber from which the majority of TDF fuel is derived is a compact material, and during the pyrolysis process, a considerable amount of tars is generated, which clog the pores and inhibit the development of the internal structure within the material. Conversely, the high heterogeneity of the raw material in the case of both RDF samples resulted in an uneven formation of the porous structure, which was mainly dependent on their fractional composition. Nevertheless, it was possible to obtain a developed internal structure, which was rich in mesopores. The spherical elements visible in the images of RDF_MW_H2O_850 are the mineral phase, which is composed mainly of silica. Wood waste with a visibly developed porous structure in the case of RDF_IW_H2O_850 can also be observed in the images. It can be anticipated that an RDF alternative fuel comprising a high proportion of waste wood and woody biomass would be the most promising material for the synthesis of porous materials.

In the case of the two samples of TDF fuel and RDF fuel obtained from industrial waste, chemically activated (see Fig. 3 TDF_KOH_800 and RDF_IW_KOH_800), notable alterations in the porous structure were observed in comparison to the physically activated samples. In the case of the RDF_IW_KOH_800 sample, the application of chemical activation resulted in an enhancement in the porosity of the sample, exhibiting a locally developed mesoporous structure as evidenced in the images. However, further investigation through sorption methods is necessary to ascertain the presence of a microporous structure.

The TDF_KOH_800 sample, which underwent chemical activation, also exhibited alterations in its structure. The images revealed the presence of an irregular porous structure on the external surface, yet it remains unclear whether the internal structure of the material underwent development during the activation process.

3.5. Porosity of produced activated carbons

To evaluate the potential applicability of adsorbents in adsorption cooling devices, the most critical parameters are the specific surface area (BET), the micropore volume, and the pore diameter, which collectively enable classification of the material as micro-, meso-, or macroporous.

The findings related to the specific surface area analysis, determined through two methods: low-temperature nitrogen adsorption and methanol adsorption at the relevant process temperatures (for both adsorption and desorption) are summarized in Tables 3 and 4.

The textural properties of the samples had shown clear differences in porosity development depending on precursor and activation method. AKPA-22 and CWH-22 exhibit very high BET surface areas (750 and 844 m^2/g) with significant micropore volumes (0.23 and 0.32 cm^3/g), indicating well-developed microporosity and narrow mean pore diameters (2.6 and 2.7 nm).

In the case of the sample synthesised by the physical method from fuel extracted from used tyres, a macroporous structure was observed on SEM images, which was also confirmed by specific surface area analyses by low-temperature gas adsorption. The obtained porous carbon material TDF_H2O_850 was characterised by a low BET specific surface area, not exceeding 100 m^2/g, and a very high pore diameter, on average 10 times higher than in other cases of synthesised carbons and about 15 times higher than commercial carbons. The literature reports that tyre waste is a good and homogeneous material, rich in carbon, with high potential when it comes to synthesising activated carbons [45]. The unsatisfactory outcomes observed in this study may be due to the insufficient residence time of the sample within the reactor or the inadequate process temperature. In comparison to the results observed for materials with a much higher degree of heterogeneity, such as alternative fuels, both RDF samples showed promising results in developing the specific surface area, which ranged from approximately 250 to 330 m^2/g. These results are not as promising as those of commercial materials [46–49]. However, it is important to note that the raw material used is a waste and methods for its efficient industrial use are continually being sought. In contrast, chemical activation yielded up to three times the active surface area of BET (in the case of the RDF_IW sample), which exceeds the values for activated carbons obtained by physical activation of pure raw materials. The sample extracted from the alternative fuel type TDF, even with the chemical method, did not develop its internal surface area, although a significant improvement was obtained compared to physical activation. One of the key obstacles, however, is the energy intensity of the chemical activation process, generating additional waste, without yielding a valuable synthesis gas.

The analysis of the micropore volume (Table 3) indicates substantial differences in the porosity of the studied materials. The highest values were obtained for CWH-22 (0.32 cm^3/g) and AKPA-22 (0.23 cm^3/g), confirming their predominantly microporous character, which is favourable for applications involving gas-phase adsorption and separation. In contrast, RDF-based samples exhibited lower micropore volumes, with RDF_MW_H_2O_850 (0.09 cm^3/g) and RDF_IW_H_2O_850 (0.08 cm^3/g) showing moderate values, suggesting a mixed micro-mesoporous structure consistent with their larger mean pore diameters (around 4 nm). The RDF_IW_KOH_800 sample, despite its very high specific surface area (955.20 m^2/g), displayed only limited micropore volume (0.04 cm^3/g), indicating that its porosity is dominated by mesopores. The lowest micropore volumes were recorded for TDF-derived materials, with TDF_KOH_800 (0.02 cm^3/g) and particularly

Table 3
Microstructural parameters of commercial and produced activated carbons determined using gas adsorption method.

Sample	Specific surface area (BET), m^2/g	T-plot micropore volume, cm^3/g	Mean pore diameter (BET), nm
AKPA−22	750.66	0.23	2.56
CWH−22	844.09	0.32	2.74
TDF_H2O_850	78.34	0.01	38.94
TDF_KOH_800	183.51	0.02	2.14
RDF_MW_H2O_850	245.56	0.09	4.22
RDF_IW_H2O_850	328.97	0.08	4.18
RDF_IW_KOH_800	955.20	0.04	3.04

Table 4
Specific surface area of BET determined by methanol adsorption under reduced pressure at two process temperatures, 30 and 60 °C.

Sample	V_m, cm^3/g	Specific surface area (BET), m^2/g	R^2
AKPA−22, 30°C	134.60	871.73	98.93
AKPA−22, 60°C	80.96	524.32	99.79
CWH−22, 30°C	146.80	950.74	99.41
CWH−22, 60°C	139.80	905.39	99.42
RDF_IW_H2O_850, 30 °C	61.25	396.65	99.96
RDF_IW_H2O_850, 60 °C	59.34	384.31	99.96
RDF_IW_KOH_800, 30 °C	217.60	1408.89	93.65
RDF_IW_KOH_800, 60 °C	223.30	1446.07	93.90
RDF_MW_H2O_850, 30 °C	41.59	269.35	99.99
RDF_MW_H2O_850, 60 °C	35.54	230.19	99.77

TDF_H₂O_850 (0.01 cm^3/g), which together with their large mean pore diameters point to a predominantly meso- and macroporous structure. These observations suggest that while CWH-22 and AKPA-22 are highly suitable for processes requiring narrow micropores, RDF- and TDF-based materials may be more applicable in sorption or catalytic processes involving larger molecules due to their mesoporous or macroporous characteristics, however with limited potential application in adsorption cooling devices.

To verify the sorption properties of the produced materials under conditions more representative of practical applications, additional specific surface area measurements were conducted using methanol, the working fluid commonly employed in activated carbon adsorption chillers.

The analysis applies the physical adsorption mechanism described by the BET equation, which assumes homogeneous filling of surface sites without significant adsorbate-adsorbate interactions. While the BET equation is typically suitable for monolayer adsorption and is most applicable to organic solvents with low boiling points, its applicability to methanol, characterised by a high polarity coefficient of 0.762 and strong adsorbate-adsorbate interactions may be limited in this context.

For the commercial and physically activated samples, the results align well with those from low-temperature gas adsorption measurements, indicating minimal influence of process temperature on the internal surface characteristics of the analysed materials.

In contrast, chemically activated samples exhibited significantly different outcomes. Their BET-specific surface area, as determined using methanol vapor adsorption, was approximately 50 % higher than that obtained from nitrogen adsorption analysis. This discrepancy is likely due to incomplete removal of the activating agent, KOH, from the porous structure during the leaching process, resulting in potential reactions between residual KOH and methanol during measurements. Consequently, the results for chemically activated samples are considered unreliable, underscoring the need for more robust sample preparation and characterisation methods to ensure accuracy.

3.6. Functional groups of the obtained chars after activation

Functional groups of studied chars after activation was analysed via Fourier transform infrared spectroscopy (FTIR). The spectra of TDF, RDF_MW and RDF_IW after steam activation in 850 °C and RDF_IW after chemical activation in KOH are presented in Fig. 4. Based on FTIR measurements, there can be noted that all activated samples do not indicate the presence of peaks from 1600 — 4000 cm^{-1}. In this area bonds from 3000 — 3700 cm^{-1} are associated to O═H stretching vibrations which is related to possible presence of H_2O [50], absence of peaks in this area revel that samples do not contain any moisture. Moreover, this phenomena confirm decomposition of oxygen-containing

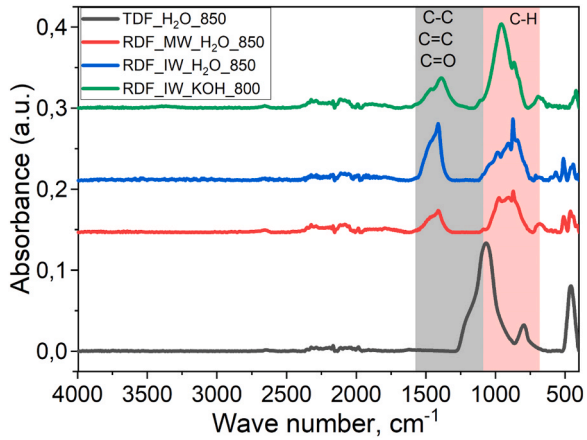

Fig. 4. FTIR spectra of activated samples: TDF, RDF_MW and RDF_IW.

structures in organic matrix of activated chars [51]. Adsorption region 1100 — 1600 cm^{-1} reveal overlapping bands related to C-C, C═C, C═O skeletal vibration bands of the carbonaceous mesh [52]. These bonds are most commonly observed in all presented RDF samples. TPF after steam activation reveal different specific spectra areas than RDF samples. In region 900 — 1200 cm^{-1}, presence of C═O valence vibration bands was identified [53], while the highest peak of 1070 cm^{-1} could reveal presence of C-O stretching vibrations [54]. Wavenumber from 700 to 1000 cm^{-1} is associated to presence of C-H bending of aromatic bonds out of plane [52]. In addition, TDF sample indicated functional group at 464 cm^{-1} associated to S-S stretching vibration [54], this kind of bond was not detected for RDF samples.

3.7. Contamination of obtained carbon porous materials with heavy metals

The contamination of activated carbons with heavy metals is a critical concern due to the potential leakage of hazardous substances, significantly restricting their potential applications. Unstable materials are unsuitable for sensitive industries such as water treatment, food processing, and pharmaceuticals.

In this study, raw waste materials: tyre-derived fuel (TDF) and two refuse-derived fuel (RDF) samples were examined alongside the final carbon-rich porous materials produced through physical and chemical activation methods. The analysis focused on the heavy metal content, its potential release, and its environmental impact. Table 5 and Fig. 5 present the heavy metal content of the as-received feedstocks, providing a comprehensive comparison to evaluate the implications for both raw and processed materials. These findings highlight the importance of addressing contamination to expand the usability of activated carbons in environmentally critical and industrial applications.

The analysis of metal content in raw feedstocks and carbon-rich waste-derived materials provides insights into the potential release of these substances into the atmosphere during the synthesis process. Zinc emerged as the predominant contaminant, warranting particular attention due to its dual significance: while essential for human health, excessive exposure to zinc can result in severe health issues affecting the nervous, cardiovascular, respiratory, reproductive, renal, and gastrointestinal systems [55].

The chemical activation process substantially reduced the zinc content in both analysed samples, suggesting partial leaching of zinc during synthesis. This finding implies that process by-products may become contaminated, raising both environmental and safety concerns. For highly contaminated precursors such as tyre-derived fuel (TDF), the proper management of waste streams generated during chemical activation is particularly critical, as it renders the process more environmentally hazardous and economically demanding. In contrast, steam activation exhibited inconsistent effects: it led to zinc accumulation in TDF_H₂O_850 and RDF_IW_H₂O_850, while a reduction was observed in RDF_MW_H₂O_850. This variability can be attributed to differences in the zinc compounds present in the raw feedstock. In municipal solid waste (MSW), zinc may occur in several chemical forms, including zinc chloride ($ZnCl_2$) and zinc oxide (ZnO), which can volatilise or transform during high-temperature activation [56].

Chromium and nickel were also identified as significant contaminants in the samples. However, in the case of both RDF-derived materials, these metals were found to be in a stable form and remained stable even after activation. This stability mitigates their potential for environmental release but highlights the need for targeted strategies to manage unstable contaminants like zinc in waste valorisation processes.

Overall, steam activation at 850 °C tends to increase the retention of metals such as Zn, Ni, Cr, Sb, and V, particularly in RDF samples. This suggests that steam activation enhances metal stabilization or reduces volatility. In contrast, chemical activation with KOH at 800 °C is more effective at reducing the retention of toxic metals like Sb, Hg, and V, while selectively enriching elements such as Cu, Co, and Mn. TDF

Table 5
Contamination of raw feedstocks and obtained carbon porous materials with selected heavy metals.

		RDF_IW	RDF_IW_H2O_850	RDF_IW_KOH_800	RDF_MW	RDF_MW_H2O_850	TDF	TDF_H2O_850	TDF_KOH_800
Zn	mg/kg	298	639	240	304	135	18 052	37 415	11 652
Ni	mg/kg	77.7	1 028	665	135	296	9.23	15.1	34.5
Cr	mg/kg	191	2332	1158	390	845	5.61	21.2	216
Cu	mg/kg	26	182	67.9	56.2	195	66.5	83.4	218
Pb	mg/kg	19.5	13.5	15.2	25.1	26.8	31.7	15.6	13.2
Co	mg/kg	10.5	9.1	41	11.7	32.2	147	124	171
Mn	mg/kg	72.3	34	355	111	399	9.67	12.2	4.8
V	mg/kg	5.89	43.1	7.96	13.9	57.1	1.97	4.2	3.19
Sb	mg/kg	43.1	358	94	30.1	13	< 1.5	0	9.77
Cd	mg/kg	0.743	1	0.136	0.4	0	0.583	0.97	0.794
As	mg/kg	< 1.0	< 1.0	< 1.0	< 1.0	< 1.0	< 1.0	< 1.0	< 1.0
Hg	mg/kg	0.074	0.035	0.536	0.638	0.005	0.012	0.008	0.007

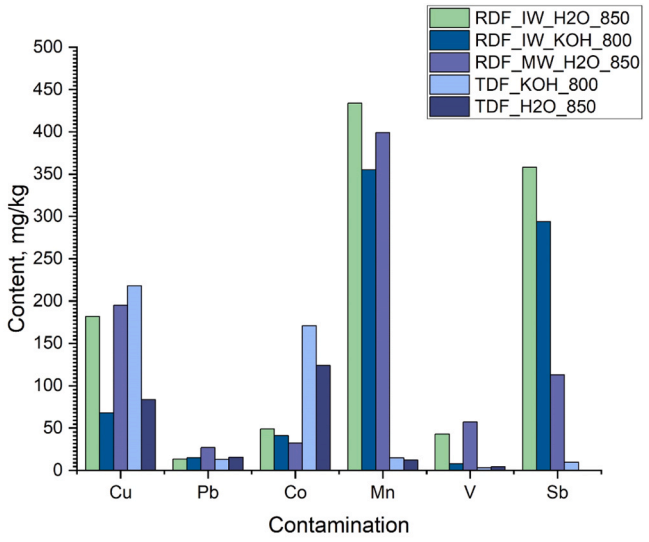

Fig. 5. Contamination of obtained carbon porous materials with selected heavy metals.

samples, in particular, show significant reductions in metal concentrations under KOH treatment, making it a promising method for minimizing environmental risks in solid residue. However, it makes synthesis waste treatment more challenging due to contamination with heavy metals.

3.8. Sorption characteristics

The methanol intake was tested at the temperatures of 30 and 60 °C, the sorption isotherms are shown in Fig. 6. The method was used to compare sorption properties between commercial and synthesised activated carbons and its potential in a working pair with methanol in an adsorption chiller.

The activated carbons AKPA-22 and CWH-22 exhibited a type I adsorption isotherm with slight H4 hysteresis, indicating a microporous structure with some split pores. Methanol adsorption capacity was high, increasing with decreasing temperature, typical for activated carbons. The highest uptake occurred at 30 °C (P/P_o = 90 %) with values of 32.14 % (AKPA-22) and 38.72 % (CWH-22). Sorption capacity showed weak temperature dependence.

Activated carbon synthesised from waste tyres via steam activation displayed a type III isotherm with significant hysteresis, indicating weak adsorbate-adsorbent interactions and dominant adsorbate-adsorbate interactions. Methanol uptake was below 10 %, likely due to insufficient pore development caused by low activation parameters.

Porous carbon from waste tyres using chemical activation showed a type II isotherm with H3 hysteresis and a methanol uptake exceeding 20 %, which is relatively low. The limited sorption properties may result from pore blockage during the initial pyrolysis stage.

Activated carbon derived from RDF via steam activation exhibited a type I isotherm with irregular behaviour and noticeable H4 hysteresis. The highest methanol uptake, 14.32 %, occurred at 30 °C (P/P_o = 90 %). Material from industrial waste RDF char via steam activation demonstrated promising sorption properties, with 25 % methanol uptake at both temperatures and noticeable H4 hysteresis, which is characteristic for commercial activated carbons [29]. The favourable sorption kinetics may be due to a larger mean pore diameter, nearly double that of commercial samples. Porous carbon from RDF_IW fuel via chemical activation had a clear type I isotherm, showing high microporosity with significant adsorption in the low-pressure range. The maximum methanol uptake exceeded 40 %, and H4 hysteresis confirmed the presence of narrow pores, including micropores. Temperature had minimal effect on sorption capacity.

3.9. Assessment of the potential application of the obtained materials in adsorption chillers

In summary, the sorption capacity of the sorbents under investigation was evaluated under the operational conditions of the adsorption chiller. The study assumed $T_{ads} = T_{cond} = 30$ °C, $T_{des} = 60$ °C and $T_{eva} = 7$ °C. A comparison was conducted between selected synthesised porous materials and the commercial activated carbons. According to the adopted methodology [29], the theoretical values of COP and SCP coefficients were determined, and the calculation results are presented in Fig. 7. The materials analysed in the article were tested for methanol sorption, and the values of the efficiency coefficients of the adsorption chiller with the analyzed working pairs were determined for different cycle times.

Analysing the data presented in Fig. 7, it should be noted that the highest SCP values are observed for the commercial activated carbons CWH-22 and AKPA-22, with the maximum SCP occurring for cycle times in the range of 1000–1200 s. In contrast, when examining the variation of COP with cycle time, the highest COP for each cycle time is observed for the RDF_IW_H2O/methanol working pair. However, for cycle times exceeding 1200 s, the COP values for methanol vapours with commercial activated carbons and those obtained from RDF_IW converge towards a similar value of 0.65. Considering both COP and SCP results, it can be concluded that sorbents obtained from industrial waste (RDF_IW) enable the adsorption chiller to operate at a performance level similar to that achieved with commercial activated carbons. In contrast, porous materials obtained from tyres (TDF) and municipal waste (RDF_MW) exhibit about 30 % lower COP and approximately 50 % lower SCP compared to the methanol/RDF_IW working pair. Based on the COP and SCP curves throughout the cycle, it should be noted that the sorption kinetics of the methanol/RDF_IW_H2O pair are more dynamic than those of the commercial activated carbons with methanol, resulting in the maximum SCP being observed within the range of 700–900 s. On the other hand, the methanol/RDF_IW_KOH working pair exhibits the

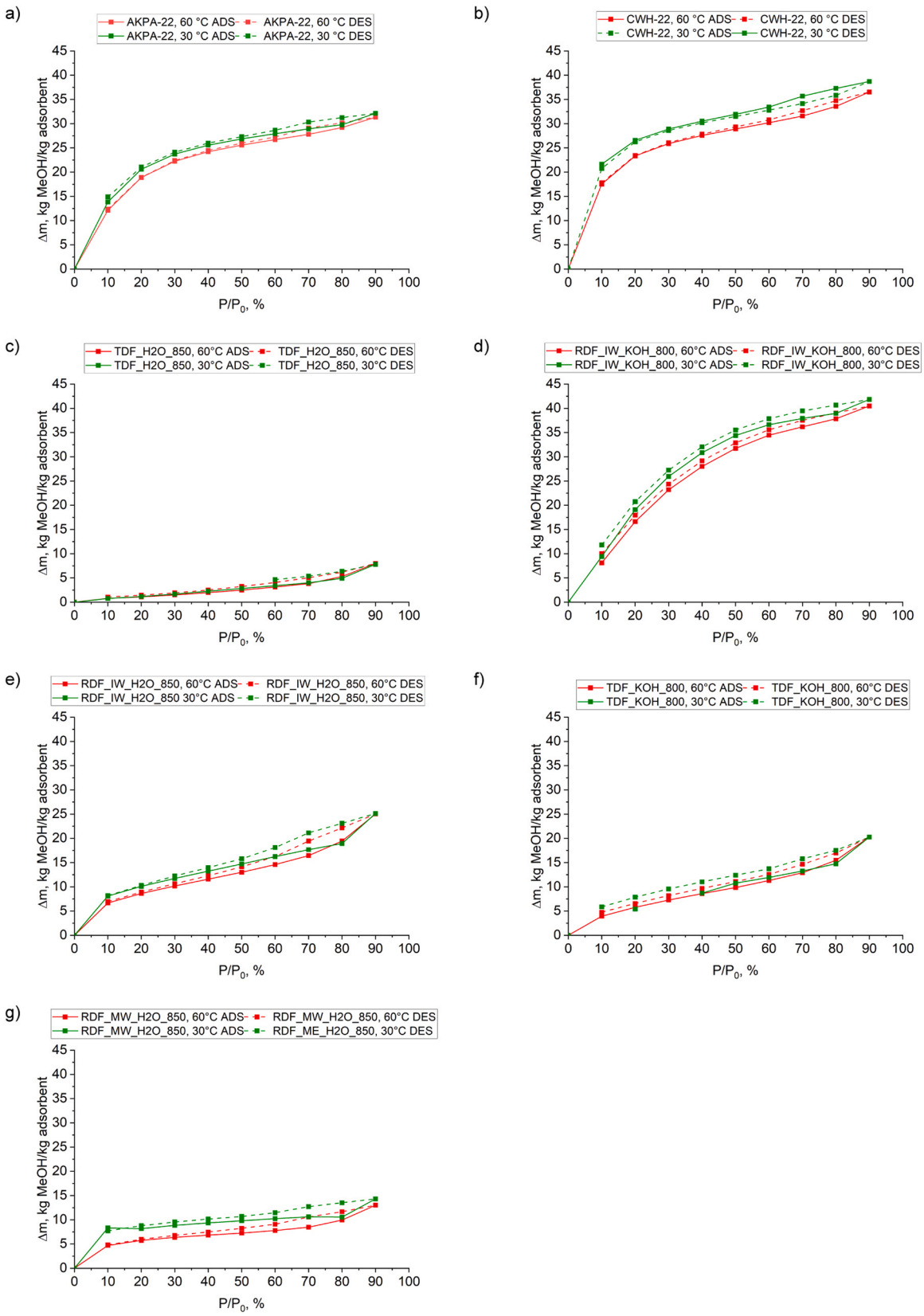

Fig. 6. Adsorption and desorption isotherms for the commercial activated carbons and obtained samples at 30°C and 60°C: a) AKPA-22, b) CWH-22, c) TDF_H2O_850, d) TDF_KOH_800, e) RDF_IW_H2O_850, f) RDF_IW_KOH_800, and g) RDF_MW_H2O_850.

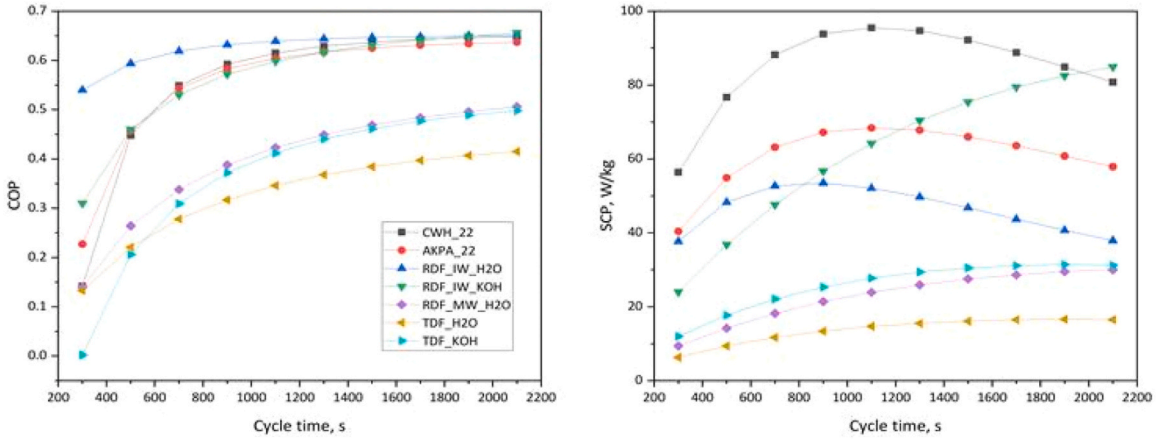

Fig. 7. Theoretical values of SCP and COP ratios for different cycle times of an adsorption chiller operating with methanol and different carbons analysed in this study.

lowest methanol sorption kinetics among the materials analysed, and for cycle times up to 2100 seconds, no maximum SCP value has been observed. It is worth noting that the greatest differences in sorption kinetics intensity occur during the desorption process. Desorption is most intense for the methanol/RDF_IW_H2O and methanol/TDF_H2O pairs, while it is slowest for the methanol/RDF_IW_KOH pair. This phenomenon may be directly related to the presence of metallic contamination in the samples. Materials with the most intense desorption kinetics show the highest metal contamination, which is nearly 4 % for TDF_H2O. In contrast, the lowest metal contamination is observed for RDF_IW_KOH, which exhibits the slowest desorption. It is worth noting that the metallic contaminants, primarily zinc, chromium, nickel, and copper, are highly thermally conductive, which directly impacts the efficiency of heat and mass transfer in sorption processes. In this context, the presence of metals in the analysed samples should not necessarily be viewed as contamination when these sorbents are used in adsorption chillers. Additionally, it is important to note that porous materials chemically activated with KOH generally exhibit slower methanol sorption compared to those activated with steam. This could be due to incomplete purging of the material, leaving residual KOH within its structure. Therefore, potassium hydroxide can react with methanol, which is characteristic of interactions between alcohols and bases. When KOH dissolves in methanol, it dissociates, forming potassium methanolate and water in an exothermic reaction. The local increase in temperature due to this reaction can slow down adsorption kinetics and even cause local desorption of already adsorbed methanol. This may be directly related to the fact that the adsorption process for KOH-activated carbons is several times longer than the desorption process. To verify these hypotheses, the synthesis of activated carbons with a modified washing step should be performed to eliminate residual KOH from the porous structure of the material. However, the significant differences in the sorption kinetics intensity of the analysed working pairs make it challenging to directly compare them. The SCP index reaches its maximum at a specific cycle time, while the COP asymptotically approaches a particular value. For this reason, 0summarizes the maximum SCP values and the corresponding COP values for the working pairs analysed in this article, as well as those studied by other research teams.

Analysing the data presented in Table 6, it can be observed that the RDF_IW_KOH/methanol pair achieves an SCP of 88.9 W/kg and a COP of 0.673 under the analysed operating conditions. In this respect, this working pair performs at a similar level to commercial activated carbons. However, the SCP_{max} and COP values must be considered in relation to sorption kinetics, as they are attained with an adsorption chiller operation cycle approximately three times longer than that of working pairs with commercial carbons, and four times longer than the RDF_IW_H2O/methanol pair. Due to this, the RDF_IW_H2O/methanol pair, which allows an SCP_{max} of 53.5 W/kg, appears to be a promising option for use in adsorption chillers. Nonetheless, the chemically activated RDF_IW sorbent still requires further optimization of the activation process to improve sorption kinetics. Additionally, it should be noted that porous materials derived from tyres exhibit significantly lower efficiencies and, when paired with methanol, do not currently represent a viable solution for adsorption chiller applications. However, it should be borne in mind that a relatively low heat source temperature of 60°C was used in the case under consideration, which allows the use of low-temperature waste heat sources. A low chilled water temperature of 7 °C was also assumed in the calculations.

Table 6
Summary of SCP and COP ratios of an adsorption chiller operating with different operating working pairs.

Working pair	T_{ads}, T_{cond}, °C	T_{des}, °C	T_{evap}, °C	SCP_{max} W/kg	COP for SCP_{max}	Reference
AC/methanol	-	110	−7	11.0	0.057	[57]
Micro-AC/ methanol	30	110	30	65.0	0.100	[58]
AC/methanol	26–28	60–70	4–5	140.0	0.570	[59]
AC/methanol	30	85	14	105.0	0.450	[60]
AC35/methanol	35	100	−2	210.2	0.329	[61]
AC MBC/ methanol	30	60	7	111.9	0.639	[29]
CWH−22/ methanol	30	60	7	95.5	0.615	This study
AKPA−22/ methanol	30	60	7	68.4	0.604	This study
RDF_IW_H2O/ methanol	30	60	7	53.5	0.631	This study
RDF_IW_KOH/ methanol	30	60	7	88.9	0.673	This study
RDF_MW_H2O/ methanol	30	60	7	30.4	0.528	This study
TDF_H2O/ methanol	30	60	7	16.6	0.411	This study
TDF_KOH/ methanol	30	60	7	31.4	0.498	This study

4. Conclusions

A comprehensive investigation into the synthesis of porous materials from waste resources has yielded several key findings. A methodology for producing activated carbon through pyrolysis and subsequent physical or chemical activation was proposed, focusing particularly on developing porous structures and generating hydrogen-rich syngas.

However, the parameters used were found to be suboptimal for treating waste tires, as they limited the formation of a well-developed porous structure. In contrast, despite the inherent heterogeneity of refuse-derived fuel (RDF) samples, the process of producing char at 600 °C followed by steam activation at 850 °C successfully facilitated the development of a porous network. The resulting specific surface areas reached 245.56 m^2/g and 328.97 m^2/g, while the maximum methanol uptakes were 14.32 for RDF_MW and 25.14 for RDF_IW, respectively. Additionally, both RDF-derived carbons demonstrated strong potential for hydrogen-rich syngas production, with nearly 70 % hydrogen detected in the syngas generated from industrial waste. Among commercial references, the highest methanol uptake was observed for CWH-22, Importantly, in the low P/P_0 region, critical for adsorption chiller applications, the chemically activated RDF_IW sample displayed adsorption isotherms comparable to those of the commercial carbons, underscoring its potential as a viable alternative sorbent.

Elemental analysis revealed chromium and nickel to be present in stable forms in RDF-derived carbons, whereas zinc persisted as a major contaminant. Partial leaching of zinc during chemical activation highlights associated environmental and health risks. Thus, effective control of zinc and other heavy metals is imperative, particularly for highly contaminated feedstocks such as TDF, to ensure both sustainability and safety of waste-derived carbons.

Performance evaluation of methanol vapor demonstrated that carbons derived from industrial waste can achieve specific cooling power (SCP) and coefficient of performance (COP) ratios comparable to those of commercial materials. Specifically, the RDF_IW_H_2O/methanol working pair exhibited a theoretical maximum specific cooling power (SCPmax) of 53.5 W/kg, while the RDF_IW_KOH/methanol pair reached 88.9 W/kg.

However, there are challenges that currently limit large-scale applications, including flow resistance, a loss of sorption properties in thicker layers, and limited cooling capacity. Therefore, future work should focus on optimizing sorbent architecture, paying particular attention to the high heterogeneity of the feedstock. Development of composite structures that enhance heat transfer and validation of these systems under near-operational conditions are also essential.

Finally, the analysis of sorption kinetics indicated that chemically activated carbons require refinement of their washing procedures. Methodological improvements in this step may significantly enhance adsorption performance, making the investigated working pairs

CRediT authorship contribution statement

Chunfei Wu: Writing – review & editing, Supervision. **Wojciech Kalawa:** Investigation. **Małgorzata Sieradzka:** Writing – original draft, Investigation. **Agata Mlonka-Mędrala:** Writing – original draft, Supervision, Resources, Project administration, Methodology, Investigation, Conceptualization. **Aneta Magdziarz:** Writing – review & editing, Supervision, Resources. **Tomasz Bujok:** Writing – original draft, Methodology, Investigation. **Marcin Sowa:** Investigation.

Declaration of Competing Interest

The authors declare that they have no known competing financial interests or personal relationships that could have appeared to influence the work reported in this paper.

Acknowledgements

This project has received funding from the European Union HORIZON TMA MSCA Staff Exchanges (HORIZON-MSCA-2021-SE-01), grant agreement no 101086071, project name “CUPOLA — Carbon-neutral pathways of recycling marine plastic waste”. Support was also provided by the Ministry of Science and Higher Education in Poland through the program "PMW grant no. 5863/HE/2024/2 (no. W52/HE/2024) and by the Ministry of Science and Higher Education, Poland (AGH grant no. 16.16.110.663 and 16.16.210.476).

Data Availability

Data will be made available on request.

References

[1] Y. Guo, C. Tan, J. Sun, W. Li, J. Zhang, C. Zhao, Porous activated carbons derived from waste sugarcane bagasse for CO2 adsorption, Chem. Eng. J. 381 (2020) 122736, https://doi.org/10.1016/j.cej.2019.122736.
[2] M.R. Ketabchi, S. Babamohammadi, W.G. Davies, M. Gorbounov, S. Masoudi Soltani, Latest advances and challenges in carbon capture using bio-based sorbents: a state-of-the-art review, Carbon Capture Sci. Technol. 6 (2023), https://doi.org/10.1016/j.ccst.2022.100087.
[3] G. Velvizhi, K. Balakumar, N.P. Shetti, E. Ahmad, K. Kishore Pant, T. M. Aminabhavi, Integrated biorefinery processes for conversion of lignocellulosic biomass to value added materials: paving a path towards circular economy, Bioresour. Technol. 343 (2022), https://doi.org/10.1016/j.biortech.2021.126151.
[4] N. Jafri, W.Y. Wong, V. Doshi, L.W. Yoon, K.H. Cheah, A review on production and characterisation of biochars for application in direct carbon fuel cells, Process Saf. Environ. Prot. 118 (2018) 152–166, https://doi.org/10.1016/j.psep.2018.06.036.
[5] S. Sundriyal, V. Shrivastav, H.D. Pham, S. Mishra, A. Deep, D.P. Dubal, Advances in bio-waste derived activated carbon for supercapacitors: trends, challenges and prospective, Resour. Conserv Recycl 169 (2021) 105548, https://doi.org/10.1016/j.resconrec.2021.105548.
[6] H. Patel, H. Weldekidan, A. Mohanty, M. Misra, Effect of physicochemical activation on CO2 adsorption of activated porous carbon derived from pine sawdust, Carbon Capture Sci. Technol. 8 (2023), https://doi.org/10.1016/j.ccst.2023.100128.
[7] Y.-H. Chiu, L.-Y. Lin, Effect of activating agents for producing activated carbon using a facile one-step synthesis with waste coffee grounds for symmetric supercapacitors, J. Taiwan Inst. Chem. Eng. 101 (2019) 177–185, https://doi.org/10.1016/j.jtice.2019.04.050.
[8] J.Y. Chen, Activated Carbon Fiber and Textiles, Elsevier Inc., 2016, https://doi.org/10.1016/C2014-0-03521-6.
[9] H. Marsh, F. Rodríguez-Reinoso, Activated Carbon, Elsevier, 2006, https://doi.org/10.1016/B978-0-08-044463-5.X5013-4.
[10] S. Sun, K. Vikrant, S. Verma, D.W. Boukhvalov, K.-H. Kim, Diaminopropane-appended activated carbons for the adsorptive removal of gaseous formaldehyde using a portable indoor air purification unit, J. Colloid Interface Sci. 653 (2024) 992–1005, https://doi.org/10.1016/j.jcis.2023.09.159.
[11] J.Y. Son, S. Choe, Y.J. Jang, H. Kim, Waste paper-derived porous carbon via microwave-assisted activation for energy storage and water purification, Chemosphere (2024) 141798, https://doi.org/10.1016/j.chemosphere.2024.141798.
[12] N. Venkatesan, A. Krishna, N.N. Fathima, Leather solid waste derived activated carbon as a potential material for various applications: a review, J. Anal. Appl. Pyrolysis 176 (2023) 106249, https://doi.org/10.1016/j.jaap.2023.106249.
[13] A.N. Shmroukh, A.H.H. Ali, S. Ookawara, Adsorption working pairs for adsorption cooling chillers: a review based on adsorption capacity and environmental impact, Renew. Sustain. Energy Rev. 50 (2015) 445–456, https://doi.org/10.1016/j.rser.2015.05.035.
[14] O. Fleker, A. Borenstein, R. Lavi, L. Benisvy, S. Ruthstein, D. Aurbach, Preparation and properties of metal organic Framework/Activated carbon composite materials, Langmuir 32 (2016) 4935–4944, https://doi.org/10.1021/acs.langmuir.6b00528.
[15] H. Wen, J. Gao, Y. Yang, M. Zhao, L. Gu, H. Yu, E. Liu, Effect of red mud on combustion behavior and heavy metal stabilization of refuse derived fuel (RDF), J. Environ. Chem. Eng. 11 (2023) 111106, https://doi.org/10.1016/j.jece.2023.111106.
[16] S. Edin Hamrahi, K. Goudarzi, M. Yaghoubi, Experimental study of the performance of a continues solar adsorption chiller using Nano-activated carbon/methanol as working pair, Sol. Energy 173 (2018) 920–927, https://doi.org/10.1016/j.solener.2018.08.030.
[17] K. Sztekler, W. Kalawa, A. Mika, M. Mlonka-Mędrala, W. Sowa, Nowak, Effect of additives on the sorption kinetics of a silica gel bed in adsorption chiller, Energies (2021) 1–13, https://doi.org/10.3390/en14041083.
[18] K. Sztekler, W. Kalawa, A.M. Medrala, W. Nowak, Ł. Mika, J. Krzywanski, K. Grabowska, M. Sosnowski, M. Debniak, The Effect of Adhesive Additives on Silica Gel Water Sorption Properties, 2020, pp. 1–15. https://doi.org/10.3390/e22030327.
[19] V.K. Mishra, P. Dasthagiri, E.A. Kumar, S. Mitra, Simulation study of R134a based vapour compression-adsorption hybrid chiller with activated carbon as adsorbent, Therm. Sci. Eng. Prog. 45 (2023) 102086, https://doi.org/10.1016/j.tsep.2023.102086.
[20] P. Youssef, S. Mahmoud, R. Al-Dadah, E. Elsayed, O. El-Samni, Numerical investigation of aluminum fumarate MOF adsorbent material for adsorption desalination/cooling application, Energy Procedia 142 (2017) 1693–1698, https://doi.org/10.1016/j.egypro.2017.12.551.
[21] M. Mikhaeil, M. Gaderer, B. Dawoud, On the development of an innovative adsorber plate heat exchanger for adsorption heat transformation processes; an

experimental and numerical study, Energy 207 (2020) 118272, https://doi.org/10.1016/j.energy.2020.118272.
[22] Q.W. Pan, R.Z. Wang, Experimental study on operating features of heat and mass recovery processes in adsorption refrigeration, Energy 135 (2017) 361–369, https://doi.org/10.1016/j.energy.2017.06.131.
[23] A. Sapienza, A. Frazzica, A. Freni, Y. Aristov, Dynamics of adsorptive systems for heat transformation, Springer International Publishing, Cham, 2018, https://doi.org/10.1007/978-3-319-51287-7.
[24] A. Mlonka-Mędrala, P. Evangelopoulos, M. Sieradzka, M. Zajemska, A. Magdziarz, Pyrolysis of agricultural waste biomass towards production of gas fuel and high-quality char: experimental and numerical investigations, Fuel 296 (2021) 120611, https://doi.org/10.1016/j.fuel.2021.120611.
[25] M. Sieradzka, C. Kirczuk, I. Kalemba-rec, A. Mlonka-mędrala, A. Magdziarz, Pyrolysis of biomass wastes into carbon materials, Energies 15 (2022), https://doi.org/10.3390/en15051941.
[26] F. Jerai, T. Miyazaki, B.B. Saha, S. Koyama, Overview of adsorption cooling system based on activated carbon - alcohol pair, Evergreen 2 (2015) 30–40, https://doi.org/10.5109/1500425.
[27] S.K. Henninger, M. Schicktanz, P.P.C. Hügenell, H. Sievers, H.M. Henning, Evaluation of methanol adsorption on activated carbons for thermally driven chillers part I: thermophysical characterisation, Int. J. Refrig. 35 (2012) 543–553, https://doi.org/10.1016/j.ijrefrig.2011.10.004.
[28] R.G. Oliveira, R.Z. Wang, T. Xian Li, Adsorption characteristic of methanol in activated carbon impregnated with lithium chloride, Chem. Eng. Technol. 33 (2010) 1679–1686, https://doi.org/10.1002/ceat.201000075.
[29] A. Mlonka-Mędrala, K. Jagodzińska, T. Bujok, W. Kalawa, T. Han, K. Sztekler, W. Nowak, Mika, Waste-Derived carbon porous materials for enhanced performance in adsorption chillers: a step toward a circular economy, Appl. Therm. Eng. 260 (2025) 124968, https://doi.org/10.1016/j.applthermaleng.2024.124968.
[30] M. Venturelli, E. Falletta, C. Pirola, F. Ferrari, M. Milani, L. Montorsi, Experimental evaluation of the pyrolysis of plastic residues and waste tires, Appl. Energy 323 (2022), https://doi.org/10.1016/j.apenergy.2022.119583.
[31] S. Aluri, A. Syed, D.W. Flick, J.D. Muzzy, C. Sievers, Pyrolysis and gasi fi cation studies of model refuse derived fuel (RDF) using thermogravimetric analysis, Fuel Process. Technol. 179 (2018) 154–166, https://doi.org/10.1016/j.fuproc.2018.06.010.
[32] I.H. Hwang, J. Kobayashi, K. Kawamoto, Characterization of products obtained from pyrolysis and steam gasification of wood waste, RDF, and RPF, Waste Manag. 34 (2014) 402–410, https://doi.org/10.1016/j.wasman.2013.10.009.
[33] M. Sieradzka, P. Rajca, M. Zajemska, A. Mlonka-Mędrala, A. Magdziarz, Prediction of gaseous products from refuse derived fuel pyrolysis using chemical modelling software - ansys Chemkin-Pro, J. Clean. Prod. 248 (2020), https://doi.org/10.1016/j.jclepro.2019.119277.
[34] C. Lin, J. Zhang, P. Zhao, Z. Wang, M. Yang, X. Cui, H. Tian, Q. Guo, Gasification of real MSW-derived hydrochar under various atmosphere and temperature, Thermochim. Acta 683 (2020) 178470, https://doi.org/10.1016/J.TCA.2019.178470.
[35] F. Tang, Y. Chi, Y. Jin, Z. Zhu, J. Ma, Gasification characteristics of a simulated waste under separate and mixed atmospheres of steam and CO2, Fuel 317 (2022), https://doi.org/10.1016/j.fuel.2022.123527.
[36] R. Alipour Moghadam, S. Yusup, W. Azlina, S. Nehzati, A. Tavasoli, Investigation on syngas production via biomass conversion through the integration of pyrolysis and air–steam gasification processes, Energy Convers. Manag 87 (2014) 670–675, https://doi.org/10.1016/j.enconman.2014.07.065.
[37] Z. Wang, M. Wu, G. Chen, M. Zhang, T. Sun, K.G. Burra, S. Guo, Y. Chen, S. Yang, Z. Li, T. Lei, A.K. Gupta, Co-pyrolysis characteristics of waste tire and maize stalk using TGA, FTIR and Py-GC/MS analysis, Fuel 337 (2023), https://doi.org/10.1016/j.fuel.2022.127206.
[38] C. Guclu, K. Alper, M. Erdem, K. Tekin, S. Karagoz, Activated carbons from co-carbonization of waste truck tires and spent tea leaves, Sustain Chem. Pharm. 21 (2021), https://doi.org/10.1016/j.scp.2021.100410.
[39] P. Ariyadejwanich, W. Tanthapanichakoon, K. Nakagawa, S.R. Mukai, H. Tamon, Preparation and characterization of mesoporous activated carbon from waste tires, 2003.
[40] L. Wang, T. Qin, J. Zhao, Y. Zhang, Z. Wu, X. Cui, G. Zhou, C. Li, L. Guo, G. Jiang, Exploring the nitrogen reservoir of biodegradable household garbage and its potential in replacing synthetic nitrogen fertilizers in China, PeerJ 10 (2022), https://doi.org/10.7717/peerj.12621.
[41] C.I. Aragón-Briceño, A.K. Pozarlik, E.A. Bramer, L. Niedzwiecki, H. Pawlak-Kruczek, G. Brem, Hydrothermal carbonization of wet biomass from nitrogen and phosphorus approach: a review, Renew. Energy 171 (2021) 401–415, https://doi.org/10.1016/j.renene.2021.02.109.
[42] L. Zhao, A. Giannis, W. Lam, S. Lin, K. Yin, G. Yuan, J. Wang, Characterization of Singapore RDF resources and analysis of their heating value, Sustain. Environ. Res. 26 (2016) 51–54, https://doi.org/10.1016/j.serj.2015.09.003.
[43] B. Krüger, A. Mrotzek, S. Wirtz, Separation of harmful impurities from refuse derived fuels (RDF) by a fluidized bed, Waste Manag. 34 (2014) 390–401, https://doi.org/10.1016/j.wasman.2013.10.021.
[44] R. Sarc, K.E. Lorber, Production, quality and quality assurance of refuse derived fuels (RDFs), Waste Manag. 33 (2013) 1825–1834, https://doi.org/10.1016/j.wasman.2013.05.004.
[45] I. Hita, M. Arabiourrutia, M. Olazar, J. Bilbao, J.M. Arandes, P. Castaño, Sánchez, opportunities and barriers for producing high quality fuels from the pyrolysis of scrap tires, Renew. Sustain. Energy Rev. 56 (2016) 745–759, https://doi.org/10.1016/j.rser.2015.11.081.
[46] L.W. Wang, R.Z. Wang, R.G. Oliveira, A review on adsorption working pairs for refrigeration, Renew. Sustain. Energy Rev. 13 (2009) 518–534, https://doi.org/10.1016/j.rser.2007.12.002.
[47] T.H. Rupam, M.A. Islam, A. Pal, A. Chakraborty, B.B. Saha, Thermodynamic property surfaces for various adsorbent/adsorbate pairs for cooling applications, Int J. Heat. Mass Transf. 144 (2019) 118579, https://doi.org/10.1016/j.ijheatmasstransfer.2019.118579.
[48] F. Shabir, M. Sultan, T. Miyazaki, B.B. Saha, A. Askalany, I. Ali, Y. Zhou, R. Ahmad, R.R. Shamshiri, Recent updates on the adsorption capacities of adsorbent-adsorbate pairs for heat transformation applications, Renew. Sustain. Energy Rev. 119 (2020) 109630, https://doi.org/10.1016/j.rser.2019.109630.
[49] Q. Yu, M. Li, X. Ji, Y. Qiu, Y. Zhu, C. Leng, Characterization and methanol adsorption of walnut-shell activated carbon prepared by KOH activation, J. Wuhan. Univ. Technol. Mater. Sci. Ed. 31 (2016) 260–268, https://doi.org/10.1007/s11595-016-1362-3.
[50] V. Gargiulo, M. Alfe, G. Ruoppolo, F. Cammarota, C.O. Rossi, V. Loise, M. Porto, P. Calandra, M. Pochylski, J. Gapinski, P. Caputo, How char from waste pyrolysis can improve bitumen characteristics and induce anti-aging effects, Colloids Surf. A Physicochem Eng. Asp. 676 (2023) 132199, https://doi.org/10.1016/j.colsurfa.2023.132199.
[51] W. Jerzak, A. Mlonka-Mędrala, N. Gao, A. Magdziarz, Potential of products from high-temperature pyrolysis of biomass and refuse-derived fuel pellets, Biomass.. Bioenergy 183 (2024) 107159, https://doi.org/10.1016/j.biombioe.2024.107159.
[52] C. Arnal, M. Alfè, V. Gargiulo, A. Ciajolo, M.U. Alzueta, Á. Millera, R. Bilbao, Characterization of Soot, in: 2013: pp. 333–362. https://doi.org/10.1007/978-1-4471-5307-8_13.
[53] J. Čespiva, M. Jadlovec, J. Výtisk, J. Serenčíšová, O. Tadeáš, S. Honus, Softwood and solid recovered fuel gasification residual chars as sorbents for flue gas Mercury capture, Environ. Technol. Innov. 29 (2023) 102970, https://doi.org/10.1016/j.eti.2022.102970.
[54] Y. Hu, Y. Xu, Q. Zhang, M. Chen, Y. Wang, G. Luo, In situ activation synthesis of tire-derived sorbents for efficient immobilization of elemental Mercury from flue gas, Chem. Eng. J. 476 (2023) 146558, https://doi.org/10.1016/j.cej.2023.146558.
[55] H. Schoofs, J. Schmit, L. Rink, Zinc toxicity: understanding the limits, Molecules 29 (2024), https://doi.org/10.3390/molecules29133130.
[56] T. Fujimori, Y. Tanino, M. Takaoka, Role of zinc in MSW Fly ash during formation of chlorinated aromatics, Environ. Sci. Technol. 45 (2011) 7678–7684, https://doi.org/10.1021/es201810u.
[57] L.W. Wang, J.Y. Wu, R.Z. Wang, Y.X. Xu, S.G. Wang, X.R. Li, Study of the performance of activated carbon-methanol adsorption systems concerning heat and mass transfer, Appl. Therm. Eng. 23 (2003) 1605–1617, https://doi.org/10.1016/S1359-4311(03)00104-2.
[58] S. Edin Hamrahi, K. Goudarzi, M. Yaghoubi, Experimental study of the performance of a continues solar adsorption chiller using Nano-activated carbon/methanol as working pair, Sol. Energy 173 (2018) 920–927, https://doi.org/10.1016/j.solener.2018.08.030.
[59] N. H Al-Maamory, N. Fadel Farman, Performance of solar adsorption cooling system using methanol and activated carbon as a working pair, J. Eng. 29 (2023) 71–85, https://doi.org/10.31026/j.eng.2023.07.05.
[60] K. Habib, B.B. Saha, S. Koyama, Study of various adsorbent–refrigerant pairs for the application of solar driven adsorption cooling in tropical climates, Appl. Therm. Eng. 72 (2014) 266–274, https://doi.org/10.1016/J.APPLTHERMALENG.2014.05.102.
[61] N. Modi, B. Pandya, Integration of evacuated solar collectors with an adsorptive ice maker for hot climate region, Energy Built Environ. (2021), https://doi.org/10.1016/j.enbenv.2021.01.001.